

## Controlled Deposition of SnS into/onto SnO<sub>2</sub> Nano-Particle Film and Application to Photoelectrochemical Cells

Daisuke Niinobe and Yuji Wada\*

Department of Material and Life Science,  
Division of Advanced Science and Biotechnology,  
Graduate School of Engineering, Osaka University,  
2-1 Yamadaoka, Suita, Osaka 565-0871

Received August 10, 2005; E-mail: ywada@mls.eng.osaka-u.ac.jp

The selective deposition of SnS into/onto SnO<sub>2</sub> nano-particle films was performed. The disposition of SnS was controlled by the pH of a source tin solution. The photocurrent of the photoelectrochemical cells using these SnS-deposited SnO<sub>2</sub> films depended on where SnS was deposited.

Nano-composite materials are attracting much interest in the possible applications to functional devices such as core-shell nano-particles for electroluminescence (EL) devices and semiconductor nano-particles coated with molecular dye or nano-particles for sensitized solar cells.<sup>1–3</sup> For fabrication of such functional devices, it is necessary to align particles and materials in an appropriate order. Therefore, methods for patterning particles and controlling the disposition of particles have been developed vigorously.<sup>3–8</sup> Although patterning methods in two-dimensions have been investigated by many researchers, research on the control of structures in the direction vertical to the substrate has been rare. However, the control and the definition of structures vertical to the substrate are required for some highly functional nano-composite devices. For example, it is necessary for utilizing a wide region of the sun spectrum in dye-sensitized solar cells to make films consisting of two different layers sensitized by two different sensitizers of which light-absorption regions are different.

Among materials applicable to nano-composite devices, large numbers of II–VI chalcogenide semiconductors have been investigated by many researchers. Although little attention has been paid to SnS among the II–VI chalcogenide semiconductors, SnS has high potential for electric devices, i.e. thermoelectric converters, electrochemical capacitors, and solar cells.<sup>9–15</sup>

In this study, we have incorporated SnS into the pores of SnO<sub>2</sub> nano-particle films by in-situ synthesis of SnS from tin(II) chloride aqueous solutions. We have also demonstrated that the deposition position of SnS into/onto a SnO<sub>2</sub> nano-particle film can be controlled by changing the pH of the source solution. By choosing the pH of a SnCl<sub>2</sub> solution for the source of SnS, SnS was successfully incorporated into a SnO<sub>2</sub> nano-

particle film; SnS can also be precipitated selectively onto the outer surface of a SnO<sub>2</sub> nano-particle film. We have also fabricated electrochemical cells with the composite films and demonstrated that the photo-response of the electrochemical cells depended on the degree of incorporation of SnS into the pores of SnO<sub>2</sub> nano-particle films.

6 mL of 15 wt % SnO<sub>2</sub> colloidal dispersion (Alfa Aesar,  $\phi \approx 15$  nm) was introduced in a mortar. It was followed by adding 0.1 mL of CH<sub>3</sub>COOH, 0.1 mL of 2,4-pentandione, 120 mg of Marporose 60MP-50 (Matsumoto Yushi Seiyaku), and 0.1 mL of Triton X-100. The resulting paste was spread on fluorine-doped tin-oxide-coated glass substrates (FTO) with a squeegee and spacing tapes, and then sintered in a furnace at 450 °C for 30 min. The thicknesses of the resulting SnO<sub>2</sub> nano-particle films were about 2  $\mu$ m. The average pore diameter of the SnO<sub>2</sub> nano-particle films estimated by the N<sub>2</sub> gas adsorption/desorption measurement was 8.1 nm.<sup>16</sup> SnS was deposited into the resulting SnO<sub>2</sub> nano-particle films for making SnS + SnO<sub>2</sub> composite film. 0.56 g of SnCl<sub>2</sub>·2H<sub>2</sub>O was dissolved in 100 mL of water, resulting in a solution of pH 1. A 0.025 M Na<sub>2</sub>S aqueous solution was prepared by dissolving Na<sub>2</sub>S·9H<sub>2</sub>O in water. For the preparation of SnS + SnO<sub>2</sub> composite film, SnO<sub>2</sub> film prepared as described above was immersed in a SnCl<sub>2</sub> solution of pH 1 at 80 °C, and then immersed in a 0.025 M Na<sub>2</sub>S aqueous solution. By repeating the set of the procedure 4 times, SnS was deposited. We denote the SnS particles as the SnS deposited at pH 1. 0.56 g of SnCl<sub>2</sub>·2H<sub>2</sub>O was dissolved in 100 mL of water. By adding small amounts of concd NaOH aq to the solutions, the pH of the solutions were adjusted to 10 or 12. We denote these solutions as tin solutions of pH 10 and pH 12, respectively. These solutions were cast on the substrates for the depositions of SnS because the deposited amounts of SnS were very low in the case of deposition by immersion of the substrates in these solutions. SnO<sub>2</sub> film on an FTO substrate was heated on a hot plate at 100 °C, and then a droplet of an aqueous solution of pH 10 or pH 12 was cast on an FTO substrates. Then, the 0.025 M Na<sub>2</sub>S solution was cast on the substrate, and the substrate was immersed in 80 °C hot water for removing salt in the film. SnS + SnO<sub>2</sub> composite films were synthesized by repeating the set of the procedure 4 times. These repeating times of the deposition processes were determined to give nearly the same absorbance at around 600 nm among these samples. We denote the SnS particles as the SnS deposited at pH 10 or 12, respectively. For X-ray diffraction (XRD) measurements, SnS was deposited on a flat glass substrate without SnO<sub>2</sub> nano-particle film by the same procedure described above. XRD measurements of the films were performed with a Rigaku RU-200B using a Cu K $\alpha$  X-ray source ( $\lambda = 1.54$  Å). The cross-sectional views of the composite films were observed by scanning electron microscopy (SEM; JEOL, JSM-6700F) and the content profiles of sulfur were obtained by energy dispersive X-ray spectroscopy (EDX) mapped with SEM. Photoelectrochemical cells were fabricated by sandwiching the resulting SnS + SnO<sub>2</sub> films on FTO substrates and Pt-coated FTO glass substrates together, and introducing an electrolyte between these substrates. The electrolyte was composed of methoxyacetonitrile containing 0.1 M LiI, 0.05 M I<sub>2</sub>, 0.5 M 4-*tert*-butylpyridine, and 0.6 M 1,2-dimethyl-3-propylimidazo-

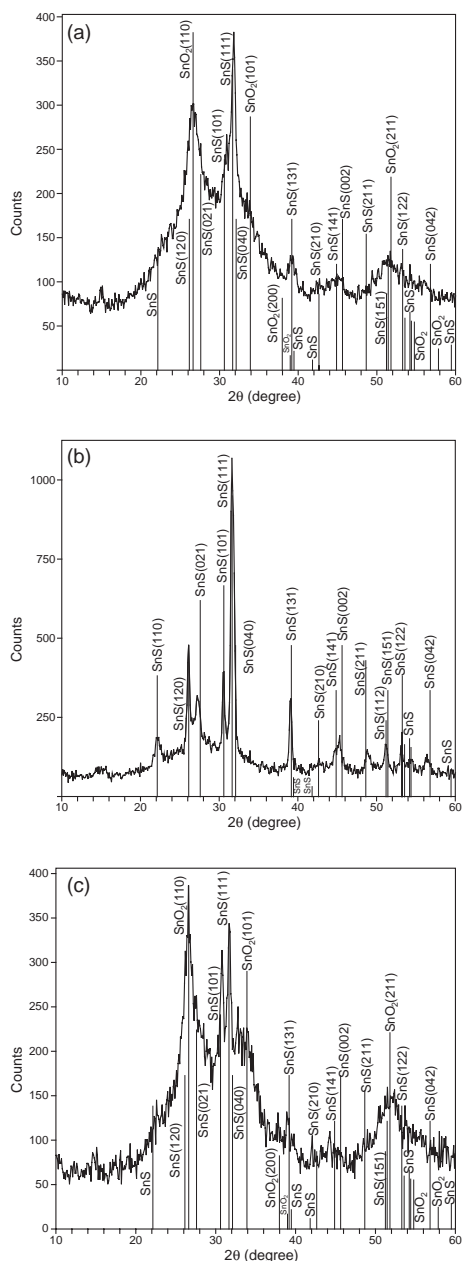


Fig. 1. XRD patterns of SnS films deposited on glass substrates from  $\text{SnCl}_2$  solutions of pH 1 (a), pH 10 (b), and pH 12 (c). The vertical bars in the figures represent the positions and intensities collected from the powder diffraction standard from JCPDS.

lithium iodide. Incident photon-to-current conversion efficiency (IPCE) was measured by a PV-25DYE (Bunko Keiki).

XRD patterns of the SnS films are illustrated in Fig. 1. In Figs. 1a and 1c, main peaks at  $2\theta = 27.5$  (021),  $30.5$  (101),  $32.0$  (111), and  $39.0$  (131) were attributed to SnS (Powder Diffraction File No. 39-0354). In Fig. 1a, the SnS(111) peak showed relatively strong diffraction, indicating that the SnS had favorable growth orientation. Broad peaks of  $26.6$  (110),  $33.9$  (101), and  $51.8$  (211) were attributed to  $\text{SnO}_2$ . In Fig. 1b, the higher diffraction intensities at  $2\theta = 22.0$  (110),  $26.0$  (120),  $30.5$  (101),  $31.5$  (111),  $32.0$  (040), and  $39.0$  (131) than those in Figs. 1a and 1c were observed. This indicated that the

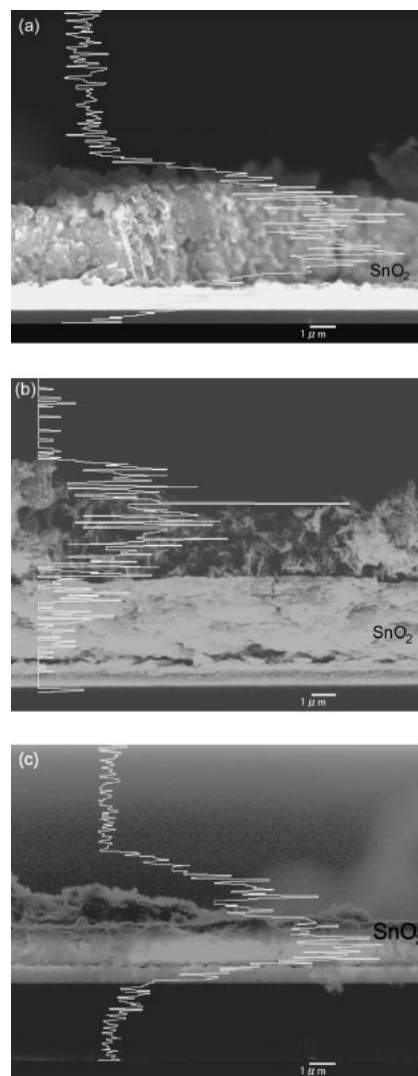


Fig. 2. Cross-sectional SEM views of SnS +  $\text{SnO}_2$  composite films deposited at pH 1 (a), pH 10 (b), and pH 12 (c) with the sulfur distribution in the film obtained by EDX (shown as white lines in the images in arbitrary unit).

SnS particles deposited at pH 10 would have better crystallinity than those deposited at pH 1 and pH 12.

White precipitates were observed in the tin solutions of pH 10. This indicated that the particles in the solution were so large as to be precipitated. The precipitates were dried and measured by XRD. The dried precipitates were attributed to  $\text{Sn}_3\text{O}_2(\text{OH})_2$  (not shown here). The particle size of the dried  $\text{Sn}_3\text{O}_2(\text{OH})_2$  estimated from the Scherrer equation was about 20 nm. Then, the SnS deposited at pH 10 would be precipitated through the reaction between  $\text{Sn}_3\text{O}_2(\text{OH})_2$  and  $\text{S}^{2-}$ . On the other hand, because the solubility of  $\text{SnCl}_2$  is high enough in an aqueous solution at low pH,<sup>17,18</sup> SnS would be precipitated from  $\text{Sn}^{2+}$  in the case of deposition from a  $\text{SnCl}_2$  solution at pH 1. Therefore, the particle size of SnS deposited at pH 1 would be smaller than that deposited at pH 10.

Figures 2a, 2b, and 2c show cross-sectional SEM views of SnS +  $\text{SnO}_2$  composite films deposited at pH 1, pH 10, and pH 12, respectively. The images contain the profiles of sulfur content obtained by EDX. It was confirmed from the homoge-

neous content profile of sulfur through the  $\text{SnO}_2$  nano-particle film in Fig. 2a that the homogeneous  $\text{SnS} + \text{SnO}_2$  composite film was successfully synthesized in the case of deposition from the  $\text{SnCl}_2$  solution at pH 1. On the other hand, the content of sulfur in Fig. 2b was higher at the outer surface of  $\text{SnO}_2$  film than in the film, which means that  $\text{SnS}$  was precipitated at the outer surface of the  $\text{SnO}_2$  nano-particle film. The difference in the deposited position of  $\text{SnS}$  could be attributed to the size of the Sn sources in the  $\text{SnCl}_2$  solutions.  $\text{SnS}$  would be precipitated from  $\text{Sn}^{2+}$  in the pores of  $\text{SnO}_2$  nano-particle films in the case of deposition from the  $\text{SnCl}_2$  solution at pH 1. Therefore,  $\text{SnS}$  would be synthesized in the pores of  $\text{SnO}_2$  nano-particle films. On the other hand, because the size of  $\text{Sn}_3\text{O}_2(\text{OH})_2$  particles precipitated from the tin solution of pH 10 was larger than that of pores of the  $\text{SnO}_2$  nano-particle film, the precipitates in the solution would not penetrate into the  $\text{SnO}_2$  nano-particle film. Therefore,  $\text{SnS}$  would be precipitated at the outer surface of  $\text{SnO}_2$  nano-particle films by reaction between  $\text{Sn}_3\text{O}_2(\text{OH})_2$  and  $\text{Na}_2\text{S}$  in the case of deposition from the tin solution of pH 10. These results indicate that the selective incorporation into the pores depending on the size of the particles<sup>19</sup> can be utilized for selective deposition of nano-particles into/onto a nano-porous film. The content profile of sulfur in Fig. 2c indicates that  $\text{SnS}$  deposited at pH 12 was deposited on both the outer surface of the film and in the pores in the  $\text{SnO}_2$  nano-particle film. This would be because there exist both a soluble species, which would be  $\text{HSnO}_2^-$ ,<sup>18</sup> and the insoluble species in the tin solution of pH 12. These findings indicated that in-situ synthesis must be carried out in a pH region of good solubility of the source metal cation for making homogeneous composite films, and metal sulfide must be precipitated from precursors larger than the size of pores for depositing particles outside of the nano-porous film.

IPCE spectra of the photoelectrochemical cells fabricated with the  $\text{SnS} + \text{SnO}_2$  composite films are shown in Fig. 3. The sensitization of  $\text{SnO}_2$  particles by  $\text{SnS}$  deposited at pH 1

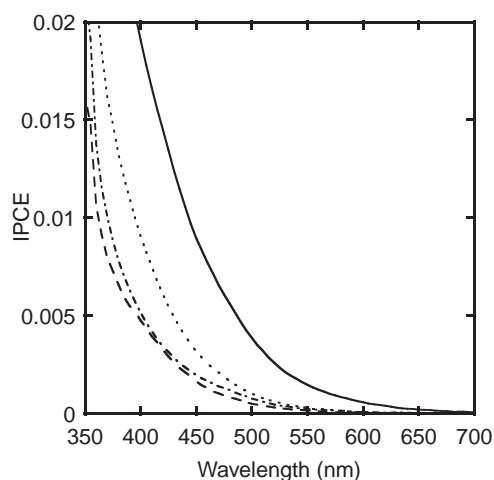


Fig. 3. IPCE spectra of the photoelectrochemical cells with the  $\text{SnO}_2$  nano-particle film sensitized by  $\text{SnS}$ . The pH of the  $\text{SnCl}_2$  solutions were pH 1 (solid line), pH 10 (broken line), and pH 12 (dotted line). The dot-dashed line indicates the IPCE of a cell with the electrode made of  $\text{SnO}_2$  nano-particle film without  $\text{SnS}$ .

was confirmed from IPCE spectra because the photocurrent response of the cell with a  $\text{SnS} + \text{SnO}_2$  composite film between 350 and 650 nm was much larger than that of the cell with a  $\text{SnO}_2$  nano-particle film without  $\text{SnS}$ . The increase of the photocurrent in the IPCE of the cell with  $\text{SnS}$  deposited at pH 1 in comparison with the other cells can be attributed to the better contact between  $\text{SnS}$  and  $\text{SnO}_2$  in the composite film.

We have successfully controlled the deposition position of  $\text{SnS}$  into/onto  $\text{SnO}_2$  nano-particle films. We have applied the film to photoelectrochemical cells, and the observed photocurrents depended on the disposition between  $\text{SnS}$  and  $\text{SnO}_2$ . This technique would be applicable to preparing a variety of composite films by changing the conditions and sizing up or down the guest particles relative to the pores. This could contribute to making tandem solar cells consisting of a nanoporous electrode and inorganic semiconductor sensitizer.

One of the authors expresses his special thanks to the center of excellence (21st Century COE) program "Creation of Integrated EcoChemistry of Osaka University."

## References

- 1 J. S. Steckel, J. P. Zimmer, S. Coe-Sullivan, N. E. Stott, V. Bulovic, M. G. Bawendi, *Angew. Chem., Int. Ed.* **2004**, 43, 2154.
- 2 B. O'Regan, M. Grätzel, *Nature* **1991**, 353, 737.
- 3 R. Vogel, P. Hoyer, H. Weller, *J. Phys. Chem.* **1994**, 98, 3183.
- 4 Y. Masuda, Y. Gao, P. Zhu, N. Shirahata, N. Saito, K. Koumoto, *J. Ceram. Soc. Jpn.* **2004**, 112, S1495.
- 5 T. Nakanishi, Y. Masuda, K. Koumoto, *Chem. Mater.* **2004**, 16, 3484.
- 6 Y. Masuda, T. Itoh, K. Koumoto, *Adv. Mater.* **2005**, 17, 841.
- 7 M. Watanabe, S. Kawaguchi, K. Nagai, *Chem. Lett.* **2004**, 33, 980.
- 8 M. Tanaka, T. Hosaka, T. Tani, I. Ohdomari, H. Nishide, *Chem. Commun.* **2004**, 978.
- 9 M. Nassary, *J. Alloys Compd.* **2005**, 398, 21.
- 10 M. Jayalakshmi, M. M. Rao, B. M. Choudary, *Electrochem. Commun.* **2004**, 6, 1119.
- 11 B. Subramanian, C. Sanjeeviraja, M. Jayachandran, *Mater. Chem. Phys.* **2001**, 71, 40.
- 12 B. Subramanian, C. Sanjeeviraja, M. Jayachandran, *Sol. Energy Mater. Sol. Cells* **2003**, 79, 57.
- 13 M. Nair, P. Nair, *J. Phys. D: Appl. Phys.* **1991**, 24, 450.
- 14 C. Estrada-Gasca, G. Alvarez-Garcia, R. Cabanillas, P. Nair, *J. Phys. D: Appl. Phys.* **1991**, 25, 1142.
- 15 M. Ristov, G. Sinadinovski, M. Mitreski, M. Ristova, *Sol. Energy Mater. Sol. Cells* **2001**, 69, 17.
- 16 S. Ito, Y. Makari, T. Kitamura, Y. Wada, S. Yanagida, *J. Mater. Chem.* **2004**, 14, 385.
- 17 J. W. Mellor, in *A Comprehensive Treatise on Inorganic and Theoretical Chemistry*, Longmans, New York, **1960**, Vol. VII, p. 427.
- 18 W. M. Latimer, in *Oxidation Potentials*, 2nd ed., Prentice-Hall, Inc., New Jersey, **1952**, p. 148.
- 19 T. Hirai, H. Okubo, I. Komasa, *J. Phys. Chem. B* **1991**, 103, 4228.